Delay-sustained pattern formation in subexcitable media

Martin Gassel,* Erik Glatt, and Friedemann Kaiser
Institute of Applied Physics, Darmstadt University of Technology, Hochschulstrasse 4a, 64289 Darmstadt, Germany
(Received 8 April 2008; published 27 June 2008)

The influence of time-delayed feedback on pattern formation in subexcitable media represented by a net of FitzHugh-Nagumo elements, a minimal model of neuronal dynamics, is studied. Without feedback, wave fronts die out after a short propagation length (subexcitable net dynamics). Applying time-delayed feedback with appropriate feedback parameters, pattern formation is sustained and the wave fronts may propagate through the whole net (signature of excitable behavior). The coherence of noise-induced patterns is significantly enhanced if feedback with appropriately chosen parameters is applied, and shows a resonancelike dependency on the delay time. In a next step, the transition to the excitable regime is investigated in dependence on the quota of elements, which get the feedback signal. It is sufficient to control approximately half of the elements to achieve excitable behavior. Regarding a medical application, where the external control of a neural tissue would affect not single neurons but clusters of neurons, the spatial correlation of the controlled elements is of importance. The selection of the elements, which get the feedback signal, is based on a spatially correlated random distribution. It is shown that the correlation length of this distribution affects the pattern formation.

DOI: 10.1103/PhysRevE.77.066220 PACS number(s): 05.45.−a, 89.75.Kd

I. INTRODUCTION

In recent decades, many investigations on the dynamics of nonlinear spatially extended systems and their control have been done. A number of them focus on the dynamics of subexcitable and excitable media. Whereas in subexcitable media excitation waves die out, the typical feature of excitable media is that wave fronts can propagate through the whole system. This excitable behavior allows signal transmission through media, being crucial for the functionality of many physical, chemical, biological, and physiological systems, e.g., the pulse propagation in neural tissues. It is well known that noise can have a constructive influence on the dynamics of nonlinear systems [1]. The existence of noise-sustained waves has been confirmed experimentally in slices of hippocampal astrocytes [2]. Alonso *et al.* showed that noise favors the emergence of spiral waves in a subexcitable Belousov-Zhabotinsky reaction [3]. Another example is the phenomenon of spatiotemporal stochastic resonance (STSR), where the most coherent patterns are found for an intermediate noise strength [4,5]. Similar to noise, variability (diversity) can crucially influence the dynamics of subexcitable media. It is shown that in a subexcitable net of FitzHugh-Nagumo (FHN) elements [6], variability can induce pattern formation [7]. The patterns are most coherent for an intermediate variability strength (variability-induced STSR).

In recent years, besides the influence of stochastic forces on nonlinear media, the control of spatiotemporal dynamics has become a topic of great interest. Time-delayed feedback is a widely used method to achieve a qualitative change in the system dynamics. Pyragas introduced a feedback control method to stabilize an unstable orbit of a chaotic attractor to control deterministic chaos [8]. In other investigations, time-delayed feedback is used to control the coherence of noise-induced oscillations [9,10] or the synchronization of two coupled oscillators [11]. In a net of oscillators, it was shown that time-delayed feedback can desynchronize the oscillators [12] or may lead to the suppression of the global oscillation [13]. It is often sufficient to control only a part of the whole net via feedback to achieve a qualitative change in the net dynamics [13,14]. Recently, the Pyragas control scheme was used to suppress pulse propagation in a chain of excitable FHN elements [15].

In the present paper, the influence of time-delayed feedback on pattern formation in a subexcitable net of FHN elements is investigated. Without feedback, wave fronts, which are either induced by special initial conditions or by additive noise, die out after a short propagation length (subexcitable net dynamics). Applying time-delayed feedback, it is shown that the wave fronts may propagate through the whole net (signature of excitable behavior). The coherence of the noise-induced patterns is significantly enhanced by the time-delayed feedback (delay-sustained pattern formation) and shows a resonancelike dependency on the delay time. In a next step, only a certain quota of all elements is controlled via the feedback. Thereby variability is introduced, because now the net contains elements with and without feedback control. It is shown that it is sufficient to control approximately half of the elements to induce excitable net dynamics. The selection of the elements that get the feedback signal is based on a spatially correlated random distribution. It is shown that the correlation length of this distribution, which determines the size of the controlled clusters, affects the pattern formation.

II. MODEL

The system under consideration is a net of $N \times N$ coupled FHN elements extended by a time-delayed feedback loop restricted to the slow variable,

$$\frac{du_{ij}}{dt} = \frac{1}{\epsilon}[u_{ij}(1-u_{ij})(u_{ij}-a) - v_{ij} + d] + D_u \nabla^2 u_{ij},$$

*martin.gassel@physik.tu-darmstadt.de

$$\frac{dv_{ij}}{dt} = u_{ij} - cv_{ij} + e + F_{ij}(K,t,\tau) + \xi_{ij}(t). \quad (1)$$

The elements are arranged on a square grid and labeled by the indices $1 \le i,j \le N$. In a neural context, $u_{ij}(t)$ represents the membrane potential of the neuron at position (i,j) and $v_{ij}(t)$ is related to the time-dependent conductance of the potassium channels in the membrane [16]. The dynamics of u is much faster than that of v. The separation of the time scales is realized by choosing the parameter value $\epsilon = 0.01$. The time is specified in time units (t.u.), where one time unit accords approximately with the duration of an excitation loop of a single FHN element. The coupling restricted to the fast variable is diffusive using a nine-point discretization of the Laplacian,

$$\nabla^2 u_{ij} = \frac{1}{6}[u_{i+1,j+1} + u_{i+1,j-1} + u_{i-1,j+1} + u_{i-1,j-1} + 4(u_{i+1,j} + u_{i-1,j} + u_{i,j+1} + u_{i,j-1}) - 20u_{ij}]. \quad (2)$$

The parameter D_u denotes the coupling strength. The feedback term, also called the feedback signal,

$$F_{ij}(K,t,\tau) = K[v_{ij}(t-\tau) - v_{ij}(t)]g_{ij}, \quad (3)$$

is introduced as in [11]. K is the feedback strength and τ is the delay time measured in time units (t.u.). Introducing the feedback signal in the fast variable u yields qualitatively the same results. The matrix element g_{ij} is either equal to 1 or equal to 0 to select the elements that get the feedback signal. We introduce the parameter g_f,

$$g_f = \sum_{i,j=1}^{N} g_{ij}/N^2, \quad 0 \le g_f \le 1, \quad (4)$$

the quota of elements that get the feedback signal. We denote the parameters K, τ, and g_f as *feedback parameters* for brevity. The feedback control scheme [Eq. (3)] is noninvasive in the sense that the feedback signal vanishes when the element remains in its fixed point.

The selection of elements that get the feedback signal is either based on a spatially uncorrelated Gaussian random distribution or on a spatially correlated Gaussian distributed variable η_{ij} with the following exponential correlation function:

$$\langle \eta_{ij}\eta_{kl}\rangle = \exp\left(-\frac{(i-k)^2 + (j-l)^2}{\lambda^2}\right), \quad (5)$$

with λ the spatial correlation length. For a given realization of η_{ij} and a fixed value of g_f, the ij element gets the feedback signal if $\eta_{ij} < \alpha$ with $H(\eta_{ij} < \alpha) = g_f$, where H denotes the distribution function of η_{ij}. In Fig. 1, the matrix elements g_{ij} are plotted for $g_f = 0.5$ and three different values of the correlation length λ. Black denotes $g_{ij} = 1$, these elements get the feedback signal, and white denotes $g_{ij} = 0$. For larger values of λ, larger clusters of elements get the feedback signal.

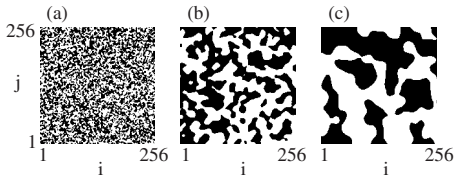

FIG. 1. The matrix elements g_{ij} for $g_f = 0.5$ and three different values of the correlation length λ. Black denotes $g_{ij} = 1$, white $g_{ij} = 0$. (a) $\lambda = 1.0$, (b) $\lambda = 5.0$, (c) $\lambda = 10.0$.

The equations are integrated on a discrete spatiotemporal grid using the Heun method ($\Delta t = 0.001$ t.u.) and the Forward Time Centered Space scheme in time and space, respectively [17]. The integration in space is performed using periodic boundary conditions.

The additive noise term $\xi_{ij}(t)$ is taken to be spatially uncorrelated Gaussian white noise with zero mean. Hence the correlation function reads

$$\langle \xi_{ij}(t)\xi_{kl}(t')\rangle = \sigma_a^2 \delta_{ij,kl}\delta(t-t'), \quad (6)$$

where σ_a denotes the noise strength.

First the dynamics of the net [Eq. (1)] is studied without feedback in dependence on the parameters c, e, and D_u, whereas the parameters $a = 0.5$, $d = 0.1$, and $N = 256$ are fixed throughout this paper. For the examined range of the parameters c and e, the single uncoupled FHN element has one stable fixed point (focus) and shows excitable dynamics. Driving the single element beyond a certain threshold leads to a large excursion through the phase space (spike in the time series) before the trajectory returns to the fixed point. The duration of a whole spike is composed mainly of the duration of the excitation spike B and the duration of the refractory period R [Fig. 2(a)]. The measure $\Delta B = B(c,e)/B(3.85,0.0)$ is introduced as the normalized time span of an excitation spike, for which $u(t) \ge 0.4$ is valid. $\Delta R = R(c,e)/R(3.85,0.0)$ [$u(t) \le 0.18$] is the normalized duration of the refractory period. Contrary to the feedback case, ΔR does not change significantly with the parameters c and e (not plotted here). Figure 2(b) shows the relative change of the duration of an excitation spike ΔB in dependence on c and e. ΔB increases with increasing values of c and decreasing values of e, but the element shows always excitable dynamics. Regarding the diffusively coupled net, however, one can discern two different dynamical regimes. In Figs. 3(a) and 3(b), snapshots of the variable $u_{ij}(t)$ are shown for different consecutive times t and fixed parameter values of e

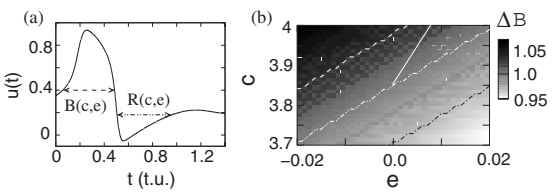

FIG. 2. (a) Sketch for the definition of the duration B of the excitation spike and the duration R of the refractory period. (b) ΔB dependent on c and e. (–·–) $\Delta B = 0.97$, (···) $\Delta B = 1.0$, (– – –) $\Delta B = 1.03$, (—) the effective parameter change (for details, see Sec. III).

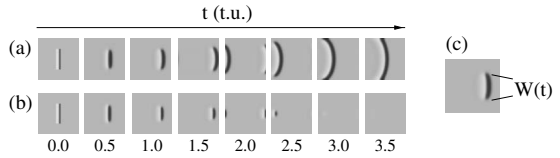

FIG. 3. (a),(b) Snapshots of the variable $u_{ij}(t)$ for different consecutive times t. (a) Excitable net dynamics ($c=4.0$). (b) Subexcitable net dynamics ($c=3.85$). The amplitude $u_{ij}(t)$ is encoded in gray scales, where white denotes the minimal and black the maximal amplitude. Further parameters: $e=0.0$, $D_u=50.0$. (c) Sketch for the definition of the width $W(t)$ of the wave front. Special initial conditions, without noise ($\sigma_a=0.0$).

$=0.0$ and $D_u=50$. The simulations are started with special initial conditions to induce a wave front (artificially induced wave front). For $c=4.0$, the wave front increases and propagates through the whole net [Fig. 3(a)], a signature of excitable behavior. For $c=3.85$, the wave front is shrinking and dies out after a finite propagation time [Fig. 3(b)]. The net shows subexcitable behavior. To determine whether the net shows excitable or subexcitable dynamics, the quotient of the width $W(t_i)$ of the wave front [Fig. 3(c)] at two different times t_i is used,

$$\Delta W = \frac{W(t_2)}{W(t_1)}, \quad t_1 = 1 \text{ t.u.}, \quad t_2 = 4 \text{ t.u.} \tag{7}$$

The time t_1 has to be small enough to ensure that the wave front is not extended over the whole net, but one has to exclude the transient. The time t_2 is chosen larger than t_1. $\Delta W > 1$ means that the wave front is growing and the net is excitable; for $\Delta W < 1$, the wave front is shrinking (subexcitable dynamics). This case differentiation is independent of the specific choice of the times t_1 and t_2, while the above-mentioned criteria for t_1 and t_2 are fulfilled. But it is important to mention that the border between subexcitable and excitable net dynamics cannot clearly be defined, because the growing or shrinking of an artificially induced wave front depends on its initialized shape and thickness. The results presented do not lose their general validity, although the border $\Delta W=1$ is only exact for the applied initial conditions [Figs. 3(a) and 3(b), $t=0.0$ t.u.]. Simulations of the net with the artificially induced wave front are performed for different parameter values of c, e, and D_u. In Fig. 4(a), the measure

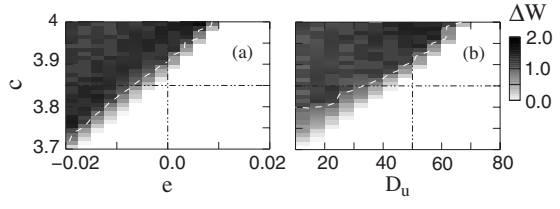

FIG. 4. ΔW in dependence on (a) c and e for $D_u=50$ and (b) c and D_u for $e=0.0$, respectively. (– – –) $\Delta W=1.0$ marks the border between the subexcitable regime (white area) and the excitable regime (gray area). (–·–·–) mark the parameter values chosen for all further simulations. Special initial conditions, without noise ($\sigma_a=0.0$).

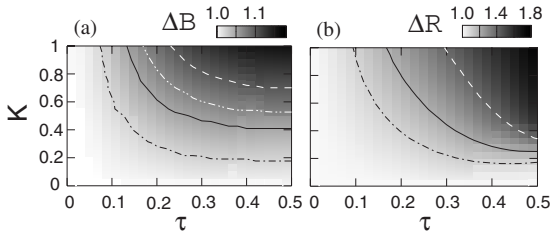

FIG. 5. (a) ΔB and (b) ΔR of a single uncoupled FHN element dependent on K and τ. (a) (–·–) $\Delta B=1.02$, (—) $\Delta B=1.05$, (···) $\Delta B=1.07$, (– – –) $\Delta B=1.1$. (b) (–·–) $\Delta R=1.1$, (—) $\Delta R=1.2$, (– – –) $\Delta R=1.4$. Special initial conditions, without noise ($\sigma_a=0.0$).

ΔW is plotted dependent on the parameters c and e for $D_u=50$. And in Fig. 4(b), ΔW is plotted dependent on the parameters c and D_u for $e=0.0$, respectively. In both panels, the dashed line ($\Delta W=1.0$) marks the border between the subexcitable (white area) and the excitable regime (gray area). The dynamics of the net depends on the parameter values c and e of the single elements and on the coupling strength. At the edge of the wave front, the elements are excited and they are performing a spike (loop in the phase space). To excite a neighboring element, which is in its fixed point, both the duration of the spike [depending on c and e, Fig. 2(a)] and the coupling strength between the elements play a crucial role. The dashed-dotted lines mark the parameter values chosen for all further simulations. For $c=3.85$, $e=0.0$, and $D_u=50$, the net is in the subexcitable regime.

III. TIME-DELAYED FEEDBACK

At first the influence of time-delayed feedback on the excitation spike of a single uncoupled FHN element is studied. In Fig. 5(a), the relative change of the duration of the excitation spike ΔB is plotted dependent on the feedback parameters K and τ. One discerns that ΔB increases with increasing parameter values of K and τ. When the element is driven from its fixed point beyond the excitation threshold, the delayed state $v(t-\tau)$ is still equal to $v_{st}=0.052$, the v coordinate of the fixed point. So at the beginning of the excitation spike, one can replace the feedback term F_{ij} in the second differential equation of Eq. (1) by introducing the effective parameters $c_{\text{eff}}=c+K$ and $e_{\text{eff}}=e+Kv_{\text{st}}$ ($c=3.85$, $e=0.0$). With an increasing value of K, the parameters c and e are effectively shifted to larger values [(—) in Fig. 2(b)], leading to an increase of the duration of the excitation spike due to the feedback signal. Regarding the whole spike, the influence of the time-delayed feedback is more complex. Besides the duration of the excitation spike, the duration of the refractory period is strongly elongated due to the feedback [Fig. 5(b)].

Next, the dynamics of the subexcitable net of FHN elements under the influence of time-delayed feedback is investigated. First the propagation of an artificially induced wave front is analyzed. Figure 6(a) shows the measure ΔW in dependence on the feedback strength K and the delay time τ, when all elements get the feedback signal ($g_f=1.0$). With increasing parameter values of K and τ, an increase of ΔW is observed. The artificially induced wave front shrinks slower and slower, since for large enough values for K and τ it starts

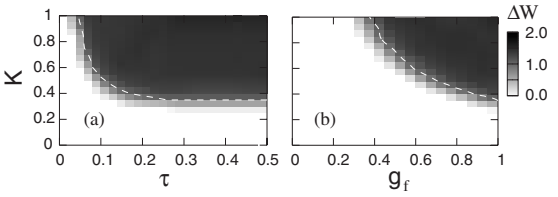

FIG. 6. ΔW in dependence on (a) K and τ for $g_f=1.0$ and (b) K and g_f for $\tau=0.3$ t.u., respectively. $\lambda=0.0$. (– – –) $\Delta W=1.0$ marks the border between the subexcitable regime (white area) and the excitable regime (gray area). Special initial conditions, without noise ($\sigma_a=0.0$).

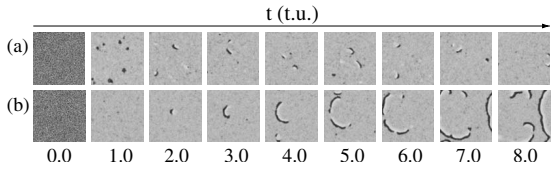

FIG. 7. Snapshots of the variable $u_{ij}(t)$ for different consecutive times t. (a) Without feedback. (b) With feedback ($K=1.0$, $\tau=0.3$ t.u., $g_f=1.0$, $\lambda=0.0$). Gray scales as in Fig. 3. Random initial conditions, with additive noise ($\sigma_a=0.1$).

growing. The dashed line ($\Delta W=1.0$) marks the border between the subexcitable (white area) and the excitable regime (gray area). As shown in Fig. 5(a), the feedback signal elongates the duration of the excitation spike of each excited element. If the duration of the excitation spike is large enough, the elements at the edge of the wave front can excite their neighboring elements and the wave front is growing and does not die out. The time-delayed feedback sustains the propagation of the artificially induced wave in the subexcitable net. For large values of τ ($\tau>0.3$ t.u.), the transition to the excitable net behavior takes place at $K=0.35$ independent of τ [see Fig. 6(a)]. This result is confirmed by further simulations up to $\tau=1.5$ t.u. In Fig. 6(b), ΔW is shown dependent on K and g_f for $\tau=0.3$ t.u. The elements that get the feedback signal are spatially uncorrelated. Again the dashed line ($\Delta W=1.0$) marks the border between the subexcitable and the excitable regime. For $K\approx 0.4$, the net shows excitable behavior if almost all elements get the feedback signal. For larger values of K, it is sufficient to control a smaller quota g_f of all elements to reach the excitable regime. An increasing K results in an increasing ΔB [Fig. 5(a)]. Consequently, for larger values of K, fewer elements at the edge of a wave front have to be controlled via the feedback signal to ensure the excitation of their neighboring elements and the propagation of an excitation wave. If K is equal to 1, only 40% of all elements have to be controlled to sustain the propagation of an artificially induced wave front.

Now the influence of the feedback signal on noise-induced pattern formation in the subexcitable net is studied. All further simulations are started with random initial conditions. Throughout this paper, the additive noise strength is fixed at $\sigma_a=0.1$. Additive noise may excite the elements and can induce wave fronts. Because of the subexcitable feature of the net, the noise-induced waves die out after a short propagation length [Fig. 7(a)]. Applying time-delayed feedback with appropriately chosen feedback parameters (e.g., $K=1.0$, $\tau=0.3$ t.u., $g_f=1.0$), the propagation of noise-induced waves is sustained [Fig. 7(b)]. Due to the feedback, which elongates the duration of the excitation spike, the excited elements are able to stimulate their neighboring elements and the noise-induced waves grow and spread out. The wave fronts propagate through the whole net, which is a signature of excitable behavior. Due to the time-delayed feedback, signal transmission through the whole net is possible, which is an important feature of neuronal networks.

To quantify the influence of the time-delayed feedback on the noise-induced patterns, the spatial cross correlation S of the variable $v_{ij}(t)$ is used [5,18]. It is defined as the space- and time-averaged nearest-neighbor amplitude distance of all elements [spatial autocovariance $C(t)$] normalized by the total spatial amplitude variance $V(t)$, which is defined as

$$V(t)=\frac{1}{N^2}\sum_{ij}(v_{ij}-\bar{v})^2,\quad \bar{v}=\sum_{i,j=1}^{N} v_{ij}. \tag{8}$$

The spatial autocovariance of the nearest neighbors can be written as

$$C(t)=\frac{1}{N^2}\sum_{ij}\frac{1}{M}\sum_{kl}(v_{ij}-\bar{v})(v_{kl}-\bar{v}), \tag{9}$$

with the indices k and l summing up all $M=4$ elements of a von Neumann neighborhood at each lattice site. The spatial cross correlation is given by

$$S=\left\langle \frac{C(t)}{V(t)}\right\rangle_T, \tag{10}$$

where $\langle\ \rangle_T$ stands for averaging over the whole integration time (a transient is excluded). S is a measure for the relative change of the local order of a spatially extended system. Thus a larger value of S denotes a greater coherence of the patterns in the net.

Another measure to quantify the coherence of the net dynamics and the transmitted information through the net is the mutual information I, an information theory-based method [19,20]. To calculate the mutual information, the spike trains of the single FHN elements have to be mapped onto a binary state space, with the states 0 and 1 corresponding to the resting and the excited state, respectively. This mapping is realized using the threshold value $u_{\mathrm{th}}=0.7$. Based on the joint Shannon entropy for several stochastic processes, the mutual information for a net of FHN elements evolving in time can be written as

$$I=\left\langle \frac{1}{M}\sum_{kl}\sum_{q,r\in\{0,1\}} p_{qr}^{ij,kl}\ln\left(\frac{p_{qr}^{ij,kl}}{p_q^{ij}p_r^{kl}}\right)\right\rangle_{ij}, \tag{11}$$

with the indices k and l summing up all $M=4$ elements of a von Neumann neighborhood at each lattice site. p_q^{ij} is the probability of the ij element to be in the state $q\in\{0,1\}$, and $p_{qr}^{ij,kl}$ denotes the joint probability of neighboring elements. The brackets $\langle\ \rangle_{ij}$ stand for averaging over all elements of the net. The mutual information I increases with an increasing interaction between neighboring elements. If one element spikes (signal) and excites a neighboring element (transmission of the signal), this pair of elements strongly interacts,

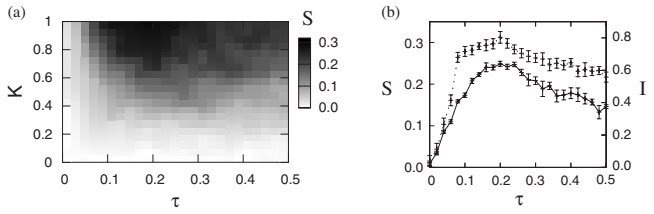

FIG. 8. (a) The spatial cross correlation S in dependence on K and τ. (b) The spatial cross correlation S (···) and the mutual information I (—) dependent on τ for $K=1$. (a),(b) Averaged over ten realizations. Random initial conditions, $g_f=1.0$, $\lambda=0.0$, $\sigma_a=0.1$.

which causes a large joint probability, and a positive contribution to I results. Regarding the whole net, the interaction between the elements provokes the development of wave fronts, which propagate through the net. The value of I increases with the number and the size of the wave fronts. Thus a larger value of I denotes a better signal transmission through the net. The mutual information takes the minimum value of zero if all elements remain in their fixed point (no excitations) or if neighboring elements spike uncorrelated.

In Fig. 8(a), the spatial cross correlation S of the noise-induced patterns is plotted dependent on the feedback parameters K and τ for $g_f=1.0$. For small values of K and τ, the noise-induced wave fronts die out very quickly, and thus the spatial cross correlation S is close to zero. The coherence of the patterns increases with increasing values of K and τ. Because of the elongated duration of the excitation spike, the probability that noise-induced wave fronts can spread out through the whole net is increased. Maximal coherent patterns are found for large values of K and $\tau \approx 0.2$ t.u.. For the case $K=1.0$, S is plotted in Fig. 8(b) dependent on τ. Increasing the value of τ leads to an elongation of the duration of the excitation spike. Noise-induced wave fronts grow and thus pattern formation in the net is sustained. But for large values of $\tau > 0.25$, the coherence of the patterns slowly decreases again. Besides an increase of ΔB [Fig. 5(a)], the feedback leads also to an elongation of the refractory period of the spike [$\Delta R > 1$, Fig. 5(b)], in which the elements are unexcitable. So for large values of τ, the propagation of waves is still sustained, but the elements remain longer in the refractory period after an excitation wave has passed them. The elongation of the refractory period means that fewer wave fronts can propagate through the net in a certain time interval. Consequently, the number of excitation waves is reduced, leading to the decrease of S. In Fig. 8(b), also the mutual information I is plotted dependent on τ ($K=1.0$). The information measure I exhibits a pronounced maximum at intermediate values of τ. Increasing the value of τ starting at $\tau=0.0$, the time-delayed feedback control allows for pattern formation and thus for signal transmission through the net. The value of I increases. For values of $\tau > 0.25$, the refractory period is strongly elongated. So less information (wave fronts) can be transmitted within a certain time. The value of I decreases again. Regarding the delay time τ, the spatial cross correlation and the mutual information show a resonancelike behavior. For an intermediate value of τ, a maximal amount of information (highest number of wave fronts) can be transmitted through the net. For even larger values of τ

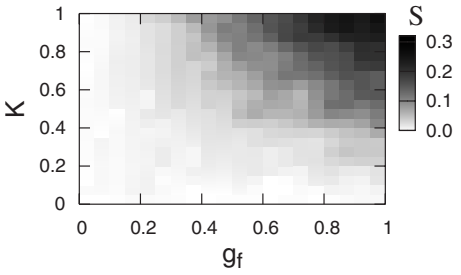

FIG. 9. The spatial cross correlation S in dependence on K and g_f for $\tau=0.3$ t.u., and $\lambda=0.0$ averaged over ten realizations. Random initial conditions, $\sigma_a=0.1$.

($0.5 < \tau \leq 1.5$ t.u.), pattern formation is sustained. The refractory period of the elements slowly increases, consequently the measures S and I slowly decrease, but no qualitative new effects occur. The feedback acts only when an excitation wave passes the elements. It vanishes while the elements remain in their fixed point. In contrast to oscillatory media, where the oscillation period ($T \approx 1.0$ t.u.) determines an intrinsic time scale for each element, in the subexcitable net a resonance effect for $\tau \approx 1.0$ t.u. does not exist.

In a next step, the quota g_f of the elements that get the feedback signal is varied, while the delay time is fixed at $\tau=0.3$ t.u., a value for which pattern formation is sustained for $K \gtrsim 0.4$. Again the selection of the elements that get the feedback signal is done spatially uncorrelated. In Fig. 9, the spatial cross correlation S of the noise-induced patterns is plotted dependent on K and g_f. The coherence of the patterns increases with increasing values of K and g_f. Again one discerns the symmetry between the influence of K and g_f on the pattern formation. For larger values of K it is sufficient to control fewer elements via the feedback signal to sustain pattern formation and vice versa [cf. Fig. 6(b)]. Again, increasing K leads to an increase of ΔB and thus fewer elements have to get the feedback signal to ensure that the excitations spread out. Nevertheless, the most coherent patterns are found if all elements get the feedback signal. To manifest this result, snapshots of the variable u_{ij} after $t=12$ t.u. dependent on K and g_f are composed in Fig. 10. For small values of K and g_f, the noise-induced waves die out very quickly. No waves or only very small wave fronts are visible in the snapshots of the net. If $K \gtrsim 0.4$ and $g_f \gtrsim 0.4$, pattern formation is sustained and the wave fronts can propagate

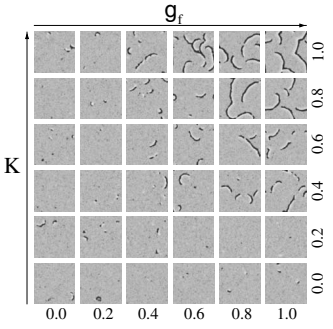

FIG. 10. Snapshots of the variable $u_{ij}(t)$ dependent on K and g_f for $\tau=0.3$ t.u., and $\lambda=0.0$. Gray scales as in Fig. 3. Random initial conditions, $\sigma_a=0.1$.

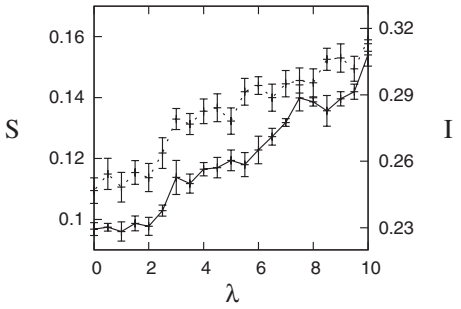

FIG. 11. The spatial cross correlation S (···) and the mutual information I (—) in dependence on λ averaged over 100 realizations. Further parameters: $\sigma_a=0.1$, $K=1.0$, $\tau=0.3$ t.u., $g_f=0.5$.

through the whole net. Comparing the first row of snapshots dependent on g_f for $K=1.0$ with the last column of snapshots dependent on K for $g_f=1.0$, the symmetry between the influence of these two feedback parameters on pattern formation is underlined.

So far for all presented results with $g_f<1.0$, the selection of the elements that get the feedback signal has been spatially uncorrelated. But regarding a medical application, where the external control of a neural tissue would affect not single neurons but clusters of neurons, the spatial correlation of the controlled elements is of importance. Consequently, the influence of the feedback control on pattern formation is studied in dependence on the spatial correlation of the controlled elements. The feedback parameters are fixed at $K=1.0$, $\tau=0.3$ t.u., and $g_f=0.5$. For this set of feedback parameters, pattern formation is sustained in the case of spatially uncorrelated feedback control. In Fig. 11, the spatial cross correlation S averaged over 100 realizations is plotted for a varying correlation length λ [Eq. (5)]. For small values of the correlation length ($\lambda\leq 2.0$), the coherence of the noise-induced patterns is independent of λ, whereas for $\lambda>2.0$, whereas the coherence S increases with increasing values of the correlation length. For increasing values of λ, larger clusters of elements get the feedback signal (Fig. 1). If the correlation length is small ($\lambda\leq 2.0$), the size of the controlled clusters is still small compared to the extension of the excitation waves and no influence of the correlation length on pattern formation is visible. This changes for larger values of λ, where the controlled clusters are of the size of the extension of the excitation waves. Within the controlled clusters, the excitation waves grow and their propagation is sustained, whereas in the regions without feedback control, the excitation waves die out. The extended clusters, which sustain pattern formation, lead to a more coherent pattern formation in the whole net. In Fig. 11, also the mutual information I is plotted in dependence on λ. I, a measure for the transmitted information, increases with increasing values of λ similar to S. Note that the presented results (Fig. 11) are the average over 100 realizations. The results of the single simulations vary quite strongly because the coherence of the noise-induced patterns depends on the realization of the spatiotemporal noise and on the randomly created clusters, which are controlled via the feedback. But nevertheless, the probability that noise-induced coherent patterns emerge and that wave fronts may propagate through the whole net increases with increasing values of λ ($\lambda>2$). So one can conclude that the clustered feedback control for large values of λ is more efficient than the spatially uncorrelated feedback control regarding the enhancement of information transmission through the net.

One can also use regular patterns to select the elements that get the feedback signal. Using a chessboard pattern, where every second element get the feedback signal ($g_f=0.5$), one gets the same results as for the case of arbitrary chosen elements ($\lambda=0$) discussed above. Nevertheless, chessboard patterns, where larger clusters of elements get the feedback signal, might have a strong influence on the pattern formation.

IV. CONCLUSIONS

In summary, we have shown that time-delayed feedback can sustain pattern formation in subexcitable media. Whereas without feedback both artificially induced wave fronts (special initial conditions) and noise-induced wave fronts die out quickly (subexcitable behavior), time-delayed feedback allows wave fronts to propagate through the whole net (excitable behavior). The feedback causes an elongation of the duration of the excitation spike of the excited elements, which then are able to excite their neighboring elements. The excitations grow and spread out through the whole net. Feedback control induces the possibility of signal transmission through the net, an important feature of neural tissues. The applied feedback scheme is noninvasive in that sense that the feedback signal tends to zero when the element remains in its fixed point. It acts only when an excitation pulse is present through a specific preparation or induced by noise. The coherence of the noise-induced patterns is significantly enhanced by the time-delayed feedback (delay-sustained pattern formation) and shows a resonancelike dependency on the delay time. Thus for an intermediate value of the delay time, a maximal amount of information (highest number of wave fronts) can be transmitted through the net.

Furthermore, pattern formation is studied, where only a quota of all elements get the feedback signal. Thereby variability is introduced, because now the net contains elements with and without feedback control. It is shown that pattern formation is sustained and that wave fronts can propagate through the whole net if at least 40% of all elements get the feedback signal. In addition to the spatially uncorrelated distribution of the elements that get the feedback signal, the influence of a spatial exponentially correlated distribution (clustered control) on pattern formation is studied. Regarding a medical application, where the external control of a neural tissue would affect not single neurons but clusters of neurons, the spatial correlation of the controlled elements is of importance. It is shown that the clustered control for large values of the correlation length is more efficient than the spatially uncorrelated feedback control regarding the enhancement of information transmission through the net.

The results presented underline that time-delayed feedback may have a crucial influence on the dynamics of spatially extended nonlinear systems. In particular, the interaction of time-delayed feedback and noise, which leads to most

coherent patterns for an intermediate delay time, might be of interest for many systems in which information transport is of importance. The delay-sustained pattern formation is studied using the paradigmatic FHN model in a rather general framework. The results are attained by a numerical integration of the full model equations. To the best of our knowledge, up to now an analytical description has not been possible. We believe that time-delayed feedback control can be used to manipulate the spatiotemporal dynamics of many other nonlinear systems in a desired manner. There might be many applications in several fields of physics, neuroscience, and biology where time-delayed feedback improves signal propagation. We hope that our investigations will contribute to the theory of extended systems under the influence of time-delayed feedback, noise, and variability and that the results can be verified in an experimental work.

ACKNOWLEDGMENTS

The authors are grateful to E. Schöll and his group, especially to M. Dahlem and F. Schneider, for stimulating discussions.

[1] F. Sagues, J. M. Sancho, and J. Garcia-Ojalvo, Rev. Mod. Phys. **79**, 829 (2007).
[2] P. Jung, A. Cornell-Bell, F. Moss, S. Kadar, J. Wang, and K. Showalter, Chaos **8**, 567 (1998).
[3] S. Alonso, F. Sagues, and J. M. Sancho, Phys. Rev. E **65**, 066107 (2002).
[4] P. Jung and G. Mayer-Kress, Phys. Rev. Lett. **74**, 2130 (1995).
[5] H. Busch and F. Kaiser, Phys. Rev. E **67**, 041105 (2003).
[6] J. S. Nagumo and S. Yoshizawa, Proc. IRE **50**, 2061 (1962).
[7] E. Glatt, M. Gassel, and F. Kaiser, Phys. Rev. E **75**, 026206 (2007).
[8] K. Pyragas, Phys. Lett. A **170**, 421 (1992).
[9] D. Goldobin, M. Rosenblum, and A. Pikovsky, Phys. Rev. E **67**, 061119 (2003).
[10] N. B. Janson, A. G. Balanov, and E. Schöll, Phys. Rev. Lett. **93**, 010601 (2004).
[11] B. Hauschildt, N. B. Janson, A. Balanov, and E. Schöll, Phys. Rev. E **74**, 051906 (2006).
[12] M. G. Rosenblum and A. S. Pikovsky, Phys. Rev. Lett. **92**, 114102 (2004).
[13] M. Gassel, E. Glatt, and F. Kaiser, Fluct. Noise Lett. **7**, L225 (2007).
[14] K. Pyragas, O. V. Popovych, and P. A. Tass, Europhys. Lett. **80**, 40002 (2007).
[15] M. Dahlem, F. Schneider, and E. Schöll, arXiv:0803.2362.
[16] J. Keener and J. Snyder, *Mathematical Physiology* (Springer, New York, 1998).
[17] J. García-Ojalvo and J. M. Sancho, *Noise in Spatially Extended Systems* (Springer, Berlin, 1999).
[18] M. T. Hütt, R. Neff, H. Busch, and F. Kaiser, Phys. Rev. E **66**, 026117 (2002).
[19] S. Yamada, M. Nakashima, K. Matsumoto, and S. Shiono, Biol. Cybern. **68**, 215 (1993).
[20] S. Yamada, M. Nakashima, K. Matsumoto, and S. Shiono, J. Neurosci. Methods **66**, 35 (1996).